



## Photon localization and Bloch symmetry breaking in luminal gratings

E. Galiffi,<sup>1</sup> M. G. Silveirinha ,<sup>2</sup> P. A. Huidobro,<sup>2</sup> and J. B. Pendry <sup>1</sup>

<sup>1</sup>*The Blackett Laboratory, Department of Physics, Imperial College London, London SW7 2AZ, United Kingdom*

<sup>2</sup>*Instituto de Telecomunicações, Instituto Superior Técnico, University of Lisbon, Avenida Rovisco Pais 1, Lisboa 1049-001, Portugal*



(Received 25 May 2021; accepted 21 June 2021; published 6 July 2021)

In gratings synthetically moving at nearly the velocity of light a symmetry breaking transition is observed between free-flowing fluidlike Bloch waves observed at lower grating velocities and, at luminal velocities, condensed, localized states of light captured in each period of the grating and locked to its velocity. We introduce a technique for calculating in this regime and use it to study the transition in detail shedding light on the critical exponents and the periodic oscillations in transmitted intensity seen in the pretransition regime.

DOI: [10.1103/PhysRevB.104.014302](https://doi.org/10.1103/PhysRevB.104.014302)

### I. INTRODUCTION

Spurred on by experimental advances in rapid modulation at optical [1,2], THz [3–5], and GHz [6] frequencies, in recent years interest has grown in systems where the parameters vary with time: in electromagnetic systems, the topic of the present paper, but also in acoustic systems [7–9]. In fact, many of the concepts are quite general and apply to any wave motion whatever the system. One of the simplest static structures is the Bragg grating whose study has shown the way to photonic crystals and to a host of other electromagnetic devices. Translational symmetry permits the analysis of gratings in terms of Bloch waves and their dispersion is characterized by a Bloch wave vector which shows band gaps: ranges of frequency within which the wave vector is complex and where light is reflected from the structure.

Localization is usually encountered in disordered systems where electron transport makes a transition from a diffusive regime, which is well understood, to a localized regime, which effectively cuts off conductivity. The transition is a complex one with no complete theoretical understanding of the localized regime and in particular of the critical exponent which is known from computer simulations [10] to be 1.571 but for which there is no fundamental derivation. However, there are other forms of localization, one of which we present here, that have a much simpler nature and are fully soluble. Their solution may shed light on the more complex problem.

We shall be concerned for the main part with a simple generalization of a Bragg grating of the form

$$\begin{aligned}\varepsilon(x - c_g t) &= \varepsilon_1 [1 + 2\alpha_\varepsilon \cos(gx - \Omega t)], \\ \mu(x - c_g t) &= \mu_1 [1 + 2\alpha_\mu \cos(gx - \Omega t)],\end{aligned}\quad (1)$$

synthetically moving with velocity  $c_g = \Omega/g$ . The velocity of light in the background medium is  $c_1 = c_0/\sqrt{\varepsilon_1\mu_1}$ . We stress that material comprising the grating does not move, rather the local properties are modulated in the synchronized form given above. This allows the structure to move with any velocity, unrestricted by the speed of light. This model has been widely adopted in time dependent studies of “space-time crystals” [11] and of nonreciprocal systems [12,13]. Closely related models have been used to study topological aspects

of so-called time crystals [14]. Although the modified grating lacks the time symmetric properties of the static case, it is parity-time (PT) symmetric and supports Bloch waves which have been the basis of previous studies. A sketch is given in Fig. 1 showing that as  $c_g \rightarrow c_1$  the forward traveling waves tend to degeneracy. Their close proximity inevitably leads to very strong interaction between the forward waves, which is responsible for their pathological Bloch symmetry breaking behavior in the luminal regime.

However, intriguingly, and the motivation of this paper, there is a range of grating velocities within which the Bloch wave picture fails and no characterization exists in terms of  $\omega(k)$ . There is a range of velocities,  $c_- < c_g < c_+$ , close to the speed of light within which light entering the medium is captured and localized inside each grating period where it is both amplified and compressed into an ever sharper pulse. The critical points  $c_-$ ,  $c_+$  define the near luminal region. In previous papers [15–17] we identified this behavior as a phenomenon where amplification is associated with compression of the lines of force which are conserved.

Here we are concerned with the approach to localization and the transition from Bloch-wave behavior to formation of localized pulses. When  $c_g < c_-$  (or  $c_g > c_+$ ) light incident on the grating excites a mixture of Bloch waves leading to periodic oscillations of intensity within the grating caused by the grating alternately adding to and subtracting energy from the waves with a period determined by the difference between speed of the Bloch waves,  $c_{\text{eff}}$ , and that of the grating. As  $c_g \rightarrow c_-$  the Bloch wave velocity also approaches  $c_-$  so that the period tends to infinity and at the same time the amplitude approaches infinity. In this way the oscillations presage the transition to localization. In fact, the period of these oscillations is related to exponential growth of energy density within the pathological region  $c_- < c_g < c_+$ . We calculate the period of these oscillations and the critical exponent with which it diverges at the transition. Within the pathological range the exponentially growing pulse will locate at a specific point within the grating period dictated by a subtle balance between its velocity keeping pace with the grating and the source of its growing energy which is also a function of location within the grating.

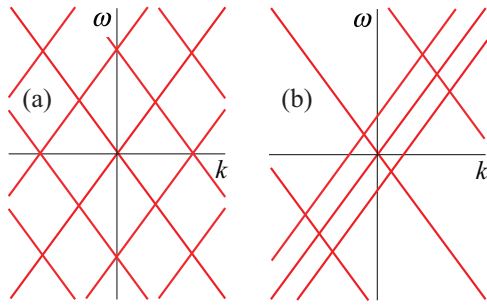


FIG. 1. (a) Dispersion of waves in a stationary grating before interaction is taken into account. (b) Dispersion of waves in a grating synthetically moving in a forward direction. Note the asymmetry between forward and backward traveling waves in (b) brought about by the lack of time reversal symmetry and the close proximity of the forward waves which collapses to a degeneracy when  $c_g = c_1$ .

The structure of our paper is as follows: first we introduce a technique for solving the equations of motion based on the “method of characteristics.” Not only does this enable efficient calculation of the grating properties, it also allows us to find analytic expressions for many of the quantities of interest. These we exploit in the next section to calculate critical exponents, prelocalization oscillations, and localization of the pulse within the critical region. Our theory holds in any scenario where backscattering is not significant.

## II. EQUATION OF MOTION

The transition to localization is essentially an interaction between forward traveling waves which are highly degenerate near the transition. Therefore to study the transition in its purest form we choose a model in which there is no backscattering so that forward and backward traveling waves, while still present, are decoupled, leaving us to concentrate on the forward waves where all the action takes place. This condition can be achieved exactly if  $\varepsilon$  and  $\mu$  are everywhere proportional,

$$\varepsilon(x - c_g t) = \mu(x - c_g t), \quad (2)$$

but is approximately true if the amplitude of the grating is sufficiently small. In the absence of backscattering the following relationships hold:

$$H_y = -\frac{1}{Z_m} E_z, \quad B_y = -Z_m D_z, \quad (3)$$

where we have assumed a wave with electric fields aligned with the  $z$  axis traveling in the forward direction along the  $x$  axis. Here,  $E_z, H_y$  are the electric and magnetic fields, and  $D_z, B_y$  are the displacement vector and magnetic induction fields, respectively. We shall exploit this result to reduce Maxwell’s equations to a partial differential equation (PDE) of the first order. Defining

$$c_g = \Omega/g = (1 + \delta)c_1 \quad (4)$$

and working in a Galilean frame comoving with the grating,  $X = x - c_g t$ , we retrieve from Maxwell

$$\frac{\partial}{\partial X} [c_\ell - c_g] D_z = -\frac{\partial}{\partial t} D_z, \quad (5)$$

with  $c_\ell = c_0/\sqrt{\varepsilon\mu}$  the local velocity of light. A fuller description of this derivation is to be found in [16]. Defining

$$\psi = [c_\ell - c_g] D_z \quad (6)$$

gives the standard form

$$(c_\ell - c_g) \frac{\partial \psi(X, t)}{\partial X} + \frac{\partial \psi(X, t)}{\partial t} = 0, \quad (7)$$

which can be solved by the method of characteristics. This approach seeks a characteristic trajectory  $X(t)$  along which  $\psi(X, t)$  is constant. Then all that is necessary to solve the PDE is to trace the trajectory back to  $t = 0$  where the value of  $\psi_0(X_0, t = 0)$  gives the value of  $\psi(X, t)$  at any subsequent time along the trajectory. To obtain the electric field we use (6) to give

$$D_z[X(t)] = \frac{c_\ell[X_0(t=0)] - c_g}{c_\ell[X(t)] - c_g} D_z[X_0(t=0)]. \quad (8)$$

The equation of motion along the trajectory is

$$\frac{dX}{dt} = (c_\ell - c_g) = c_1 \left( \frac{1}{1 + 2\alpha \cos(gX)} - (1 + \delta) \right), \quad (9)$$

which can be solved for the time at which the trajectory reaches point  $X$ , by integration,

$$\int_{X_0}^X \frac{1}{c_\ell[X'] - c_g} dX' = t(X). \quad (10)$$

For a grating with a sinusoidal profile, shown in (1), one finds

$$\begin{aligned} \theta(X) = t(X) - t_0 &= \frac{-gX}{c_1 g(1 + \delta)} - \frac{1}{c_1 g(1 + \delta)^2} \frac{2}{\sqrt{\left(\frac{\delta}{1 + \delta}\right)^2 - 4\alpha^2}} \tan^{-1} \left[ \frac{\left(\frac{\delta}{1 + \delta} - 2\alpha\right) \tan(gX/2)}{\sqrt{\left(\frac{\delta}{1 + \delta}\right)^2 - 4\alpha^2}} \right], \\ &\left| \frac{\delta}{1 + \delta} \right| > |2\alpha|, \\ &= \frac{-gX}{c_1 g(1 + \delta)} - \frac{1}{c_1 g(1 + \delta)^2} \frac{2}{\sqrt{4\alpha^2 - \left(\frac{\delta}{1 + \delta}\right)^2}} \operatorname{ctnh}^{-1} \frac{\left(2\alpha - \frac{\delta}{1 + \delta}\right) \tan(gX/2)}{\sqrt{4\alpha^2 - \left(\frac{\delta}{1 + \delta}\right)^2}}, \\ &\left| \frac{\delta}{1 + \delta} \right| < |2\alpha|, \quad \left| \left(2\alpha - \frac{\delta}{1 + \delta}\right) \tan(gX/2) \right| > \sqrt{4\alpha^2 - \left(\frac{\delta}{1 + \delta}\right)^2}. \end{aligned} \quad (11)$$

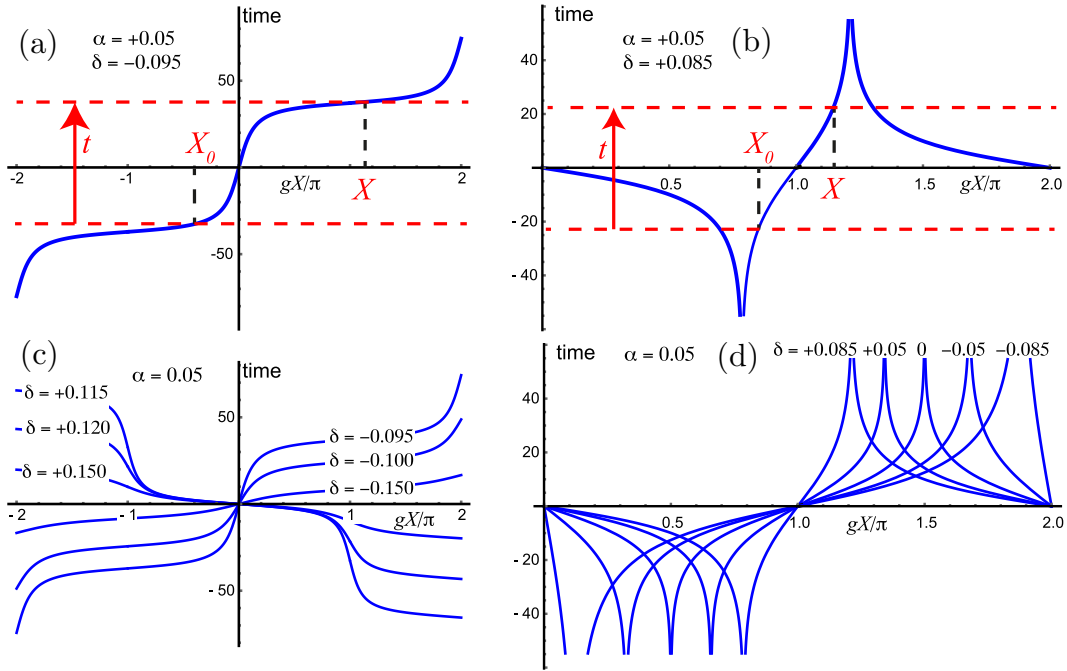


FIG. 2. The time trajectories  $t(X)$  as functions of  $X$ . (a),(c) Outside the critical velocity range,  $|\delta/1 + \delta| > |2\alpha|$ . (b),(d) Inside the critical points,  $|\delta/1 + \delta| < |2\alpha|$ . The trajectories start at a generic  $X_0$  where the value of  $\psi$  is defined. This value, constant along the trajectory, travels to point  $X$  after a time  $t$ . Panels (a) and (b) illustrate the construction for tracing time back along a trajectory to the origin: the red lines show a simple construction for finding  $X$ . Panels (c) and (d) show evolution of the trajectories with  $\delta$  which defines the difference of the grating velocity of the average velocity of light. Note that the trajectories on the left are continuous and the ones on the right are singular, implying localization.

Evidently there are critical values of  $2\alpha = \pm\delta/(1 + \delta)$  which in turn through  $\delta$  define the critical velocities  $c_-, c_+$ . The trajectories shown in Fig. 2 reveal the localization transition. When the grating velocity is outside the critical points [Figs. 2(a) and 2(c)] these trajectories show a pulse of light advancing continuously through the grating structure, albeit in the backwards direction if  $c_g > c_\ell$ . Note also that the light pauses at certain positions within the grating: at  $gX = 0$  for a subluminal grating ( $\delta < 0$ ) where the local light velocity is a minimum, and at  $gX = \pi$  for a superluminal grating ( $\delta > 0$ ) where the local light velocity is a maximum. In contrast for near luminal gratings with velocities inside the critical points [Figs. 2(b) and 2(d)] all trajectories show singularities which trap the light near that particular position. The singular points occur where the local velocity of light is the same as that of the grating and migrate to  $gX = 0, \pi$  at either end of the critical zone, to coincide with the pause zones of Figs. 2(a) and 2(c).

The curves in Fig. 2(c) show how the extra luminal curves steepen at the origin for the subluminal case and at  $gX/\pi = 1.0$  for the superluminal case. In Fig. 2(d) the singularities migrate across the unit cell with increasing  $\delta$ .

We make use of (5) to calculate a dispersion relationship assuming a time dependence of  $e^{-i\omega't'}$  in the grating frame for the Bloch wave, and arrive at

$$\frac{\partial}{\partial X} \ln[c_\ell - c_g] + \frac{\partial}{\partial X} \ln D_z = \frac{i\omega'}{c_\ell - c_g} \quad (12)$$

from which we deduce the change of phase across one unit cell which we equate to

$$k_{\text{eff}} \frac{2\pi}{g} = \omega' \int_{X_0}^{X_0 + 2\pi/g} \frac{1}{c_\ell(X) - c_g} dX = \omega' t(X_0 + 2\pi/g), \quad (13)$$

where  $k_{\text{eff}}$  is the Bloch wave vector and  $t(X_0 + 2\pi/g)$  can be found from (11),

$$k_{\text{eff}} = -\frac{\omega + c_g k_{\text{eff}}}{c_g} \left[ 1 \pm \frac{1}{\sqrt{\delta^2 - 4\alpha^2(1 + \delta)^2}} \right], \quad (14)$$

where we have substituted the frequency in the stationary frame. Solving for  $k_{\text{eff}}$ ,

$$k_{\text{eff}} = \frac{\omega}{c_1} \frac{1 \pm \sqrt{\delta^2 - 4\alpha^2(1 + \delta)^2}}{1 + \delta} \quad (15)$$

to give the effective velocity

$$c_{\text{eff}} = c_1 \frac{1 + \delta}{1 \pm \sqrt{\delta^2 - 4\alpha^2(1 + \delta)^2}}, \quad (16)$$

where we choose the “+” sign when  $\delta > 0$  and the “−” sign when  $\delta < 0$ . At the critical values of  $\alpha$ ,  $c_{\text{eff}}$  has a square root singularity as  $c_{\text{eff}} \rightarrow c_g$  and the Bloch wave locks onto the grating. The variation of  $c_{\text{eff}}$  with  $\delta$  is shown in Fig. 3. Note the shaded region within which Bloch waves are not defined, and the coincidence of  $c_{\text{eff}}$  and  $c_g$  at the critical points as

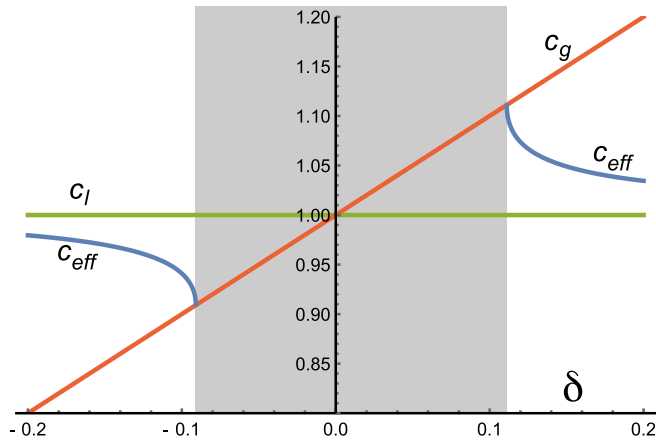


FIG. 3. The variation of  $c_{\text{eff}}$  with  $\delta$  for  $\alpha = 0.05$ , also showing the grating velocity  $c_g = 1 + \delta$  and the velocity of light in the background medium,  $c_l$ . Shading shows the range of  $\delta$  within which Bloch waves are not defined.

the grating captures and localizes the light. Below the lower cutoff  $c_{\text{eff}} < c_l$ , contrary to the predictions of Fresnel drag in a medium that is actually moving as observed in [13]. However, above the upper cutoff  $c_{\text{eff}} > c_l$ . A better predictor of  $c_{\text{eff}}$  in

$$gX_0 = -2 \arctan \frac{\sqrt{\left(\frac{\delta}{1+\delta}\right)^2 - 4\alpha^2}}{\frac{\delta}{1+\delta} - 2\alpha} \tan \left[ \frac{\theta(X) - t}{2} c_l g (1 + \delta)^2 \sqrt{\left(\frac{\delta}{1+\delta}\right)^2 - 4\alpha^2} \right], \quad (17)$$

which is then used to calculate the fields

$$\begin{aligned} D_z(X, t) &= \frac{c_\ell[X_0(t)] - c_g}{c_\ell(X) - c_g} D_{z0} \\ &= \frac{1 + 2\alpha \cos(gX)}{\frac{\delta}{1+\delta} + 2\alpha \cos(gX)} \frac{\frac{\delta}{1+\delta} + 2\alpha \cos[gX_0(t)]}{1 + 2\alpha \cos[gX_0(t)]} D_{z0}, \end{aligned} \quad (18)$$

where  $D_{z0}$  is the initial field amplitude at  $t = 0$ .

The ratio of numerator to denominator in this equation neatly expresses the compression of lines of force reported in an earlier paper [16]: the slower the velocity of waves relative to the grating the denser the lines of force, just as motorway traffic increases in density at slower speeds.

By examining the argument of  $\tan$  in (17) we deduce that the solution is oscillatory with a period given by the difference between  $c_{\text{eff}}$  and  $c_g$ ,

$$\Delta t = \frac{2\pi}{c_l g (1 + \delta)^2 \sqrt{\left(\frac{\delta}{1+\delta}\right)^2 - 4\alpha^2}}. \quad (19)$$

our example is that it is attracted to the velocity of the grating, increasingly so as the cutoff points are approached. Another interesting aspect is that  $c_{\text{eff}}$ , which serves as both the phase and group velocity of the Bloch wave, is superluminal when  $c_g > c_l$ . This may happen only in systems operating a gain mechanism.

However, this simple effective medium picture hides a wealth of structure that we shall now investigate.

### III. APPROACH TO CRITICALITY

Using the characteristic trajectories, we can easily find analytic solutions. There are two boundary conditions that could be imposed. In the first type the grating is turned on instantly everywhere; in the second the grating is turned on at a certain position in space and off at another. The latter is in fact a transmission calculation.

The boundary condition we have imposed requires the grating to be switched on at  $t = t_0$ , but if instead the light is entering a grating at some fixed point in space, the grating will be turned on at a time  $t_0 - c_g^{-1}X_0$  and off at a time  $t - c_g^{-1}X$ . This small change in the boundary conditions means that (2) is now explicitly soluble.

First consider the case outside the critical region. Using Eq. (11) we calculate

It has a maximum amplitude when  $\delta < 0$  at  $gX = \pi$ , and when  $\delta > 0$  at  $gX = 0$ ,

$$D_{z,\text{max}} = \frac{1 + \frac{\delta}{1+\delta} - \text{sgn}(\delta)2\alpha}{\frac{\delta}{1+\delta} - \text{sgn}(\delta)2\alpha} \frac{\frac{\delta}{1+\delta} + \text{sgn}(\delta)2\alpha}{1 + \frac{\delta}{1+\delta} + \text{sgn}(\delta)2\alpha} D_{z0}. \quad (20)$$

As the critical point is approached  $\Delta t$  diverges with a critical exponent of  $\nu = -1/2$  and  $D_{z,\text{max}} \rightarrow \infty$  with an exponent of  $\tau = -1$ .

These oscillations are displayed in Fig. 4(a) for a value of  $c_g$  above the critical velocity. Below in Fig. 4(b) we plot  $\varepsilon$  as defined in Eq. (1). The value of  $\varepsilon$  where  $c_g = c_\ell$ , shown notionally in the figure, is not found anywhere within the grating but  $c_\ell$  is closest to  $c_g$  in the center of Fig. 4(b). Therefore as the pulse moves to the left being overtaken by the grating it is first amplified slowing down as it moves until at  $gX/\pi = 1.0$  it reaches its minimum velocity relative to the grating, after which it accelerates away, losing energy as it goes. In Fig. 4(c) oscillations are shown for  $c_g$  below the critical velocity. Here the pulse moves to the right as it overtakes the grating, gaining energy, and traveling ever more slowly until it reaches  $gX/\pi = 0.0$  whereafter it accelerates away and loses energy. The variation of  $\varepsilon$  is shown below in

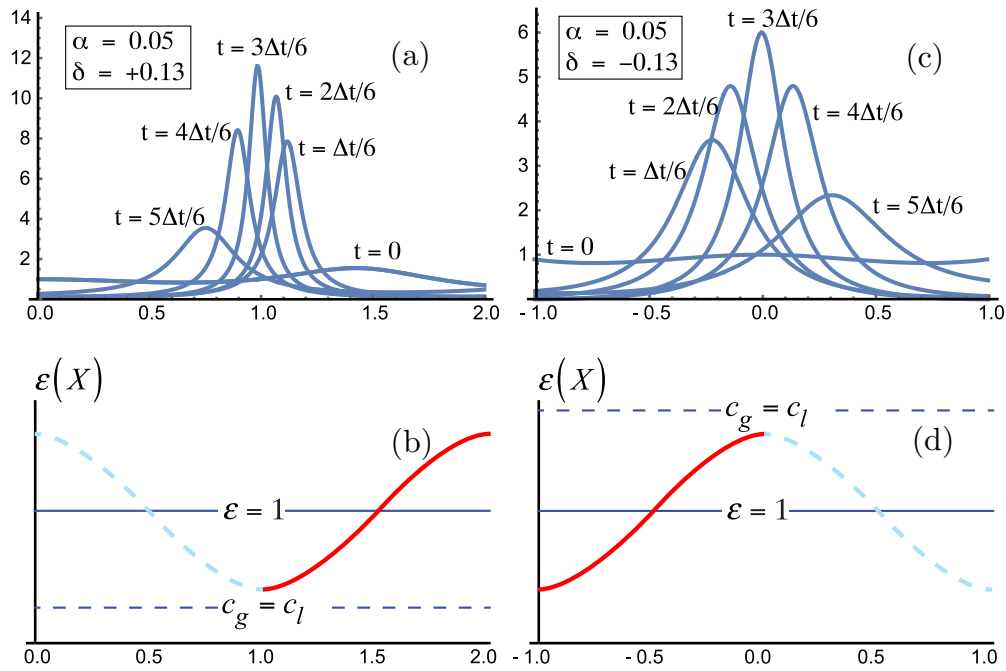


FIG. 4. Oscillations shown by (a) super- and (c) subluminal gratings plotted against  $gX/\pi$ . The times are given as fractions of the period  $\Delta t$ , as defined in (19). Below in (b) and (d) we show the variation of  $\varepsilon$  across the grating and the dashed lines show schematically the values of  $\varepsilon$  for which the grating and light velocities would be equal. The full line shows where gain occurs and dashed line shows where there is loss. Note the change of origin of the  $X$  axis between (a),(b) and (c),(d) and that for this figure  $\varepsilon_1 = 1$ .

Fig. 4(d). Our analytic theory has been verified by comparison with transfer matrix computations.

Next consider the case inside the critical region. Here from Eq. (11) we find

$$\tan(gX_0/2) = + \frac{A - e^{-tc_1g(1+\delta)^2\alpha} \left[ \frac{A}{B} - \tan(gX/2) \right] \left[ \frac{A}{B} + \tan(gX/2) \right]^{-1} + 1}{B + e^{-tc_1g(1+\delta)^2\alpha} \left[ \frac{A}{B} - \tan(gX/2) \right] \left[ \frac{A}{B} + \tan(gX/2) \right]^{-1} + 1},$$

$$A = \sqrt{4\alpha^2 - \left( \frac{\delta}{1+\delta} \right)^2}, \quad B = 2\alpha - \frac{\delta}{1+\delta} \quad (21)$$

from which, using (18), we calculate the fields shown in Fig. 5 for various values of the grating speed. In this paper we are interested in the approach to criticality: the upper critical velocity sees the maximum amplitude migrate to  $gX = \pi$  and for the lower critical velocity to  $gX = 2\pi$ . Here they meet up with the peak amplitudes outside the near luminal region.

Next we ask how the amplitude varies as the transition is approached from the localized side. For example, at the upper critical limit,

$$\lim_{t \rightarrow \infty} D_{z \max}(X, t) \approx \frac{\alpha e^{+tc_1g(1+\delta)^2\sqrt{4\alpha^2 - \left( \frac{\delta}{1+\delta} \right)^2}}}{2\alpha - \frac{\delta}{1+\delta}} D_{z0},$$

$$\frac{\delta}{1+\delta} \rightarrow +2\alpha. \quad (22)$$

Note that the exponent corresponds to the analytic continuation of the limit of the oscillation period on the other side of the transition, given in (19).

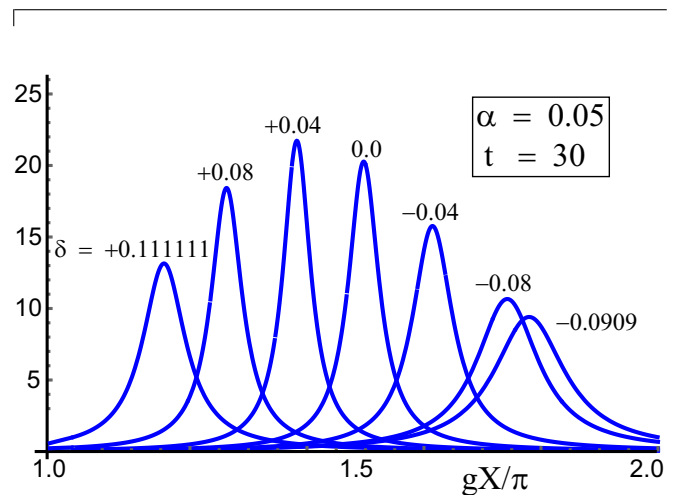


FIG. 5. Amplitude of the fields ejected from the latter half of the grating in the near luminal regime for various values of the grating speed,  $c_g = c_1(1 + \delta)$ . The critical values for this example are  $\delta = +0.111\dots$ , and  $\delta = -0.0909\dots$

#### IV. CONCLUSIONS

We have examined in detail the breaking of Bloch symmetry in a near luminal grating. The method of characteristics enables exact solution in a situation where forward scattering dominates. The latter comes about from the near degeneracy of forward traveling waves as  $c_g \rightarrow c_1$ . We observed oscillations in the transmission current in the Bloch regime with a period explained by the difference between  $c_g$  and the effective Bloch group velocity  $c_{\text{eff}}$ , the wave being alternately compressed and decompressed as it rides over different sections of the unit cell. The critical exponent of  $1/2$  with which the relative velocity of the wave and the grating vanishes at the transition point is reflected on the luminal side of the transition in the same critical exponent with which the exponential increase of amplitude growth initiates. In summary, a detailed understanding has been found of the Bloch symmetry breaking transition observed in luminal structures.

As to practical realization of these systems, apart from rf, systems graphene is a promising candidate for THz frequencies. It is known that the conductivity of graphene can be modulated at rates exceeding 100 GHz via both electro-optic [4] and all-optical mechanisms [5] and the THz surface plas-

mons of graphene may be the first excitations to be amplified in this fashion. We have previously suggested double layer graphene as a possible candidate [15].

#### ACKNOWLEDGMENTS

P.A.H. and M.S. acknowledge funding from Fundação para a Ciência e a Tecnologia and Instituto de Telecomunicações under Project No. UIDB/EEA/50008/2020. P.A.H. was supported by the CEEC Individual program from Fundação para a Ciência e a Tecnologia and Instituto de Telecomunicações by Reference No. CEECIND/02947/2020. M.S. acknowledges support from the IET under the A F Harvey Prize and by the Simons Foundation under Award No. 733700 (Simons Collaboration in Mathematics and Physics, “Harnessing Universal Symmetry Concepts for Extreme Wave Phenomena”). E.G. acknowledges support from the Engineering and Physical Sciences Research Council through the Centre for Doctoral Training in Theory and Simulation of Materials (Grant No. EP/L015579/1) and an EPSRC Doctoral Prize Fellowship (Grant No. EP/T51780X/1). J.B.P. acknowledges funding from the Gordon and Betty Moore Foundation.

- 
- [1] V. Bruno, C. DeVault, S. Vezzoli, Z. Kudyshev, T. Huq, S. Mignuzzi, A. Jacassi, S. Saha, Y. D. Shah, S. A. Maier *et al.*, *Phys. Rev. Lett.* **124**, 043902 (2020).
  - [2] H. Lira, Z. Yu, S. Fan, and M. Lipson, *Phys. Rev. Lett.* **109**, 033901 (2012).
  - [3] A. C. Tasolamprou *et al.*, *ACS Photonics* **6**, 720 (2019).
  - [4] C. T. Phare, Y.-H. D. Lee, J. Cardenas, and M. Lipson, *Nat. Photonics* **9**, 511 (2015).
  - [5] W. Li *et al.*, *Nano Lett.* **14**, 955 (2014).
  - [6] L. Planat *et al.*, *Phys. Rev. X* **10**, 021021 (2020).
  - [7] T. T. Koutserimpas and R. Fleury, *Phys. Rev. Lett.* **120**, 087401 (2018).
  - [8] V. Bacot, G. Durey, A. Eddi, M. Fink, and E. Fort, *Proc. Natl. Acad. Sci. USA* **116**, 8809 (2019).
  - [9] C. Cho, X. Wen, N. Park, and J. Li, *Nat. Commun.* **11**, 251 (2020).
  - [10] K. Slevin and T. Ohtsuki, *New J. Phys.* **16**, 015012 (2014).
  - [11] Z.-L. Deck-Léger, N. Chamanara, M. Skorobogatiy, M. G. Silveirinha, and C. Caloz, *Adv. Photonics* **1**, 056002 (2019).
  - [12] D. L. Sounas and A. Alù, *Nat. Photonics* **11**, 774 (2017).
  - [13] P. A. Huidobro, E. Galiffi, S. Guenneau, R. V. Craster, and J. B. Pendry, *Proc. Natl. Acad. Sci. USA* **116**, 24943 (2019).
  - [14] E. Lustig, Y. Sharabi, and M. Segev, *Optica* **5**, 1390 (2018).
  - [15] E. Galiffi, P. A. Huidobro, and J. B. Pendry, *Phys. Rev. Lett.* **123**, 206101 (2019).
  - [16] J. B. Pendry, P. A. Huidobro, and E. Galiffi, *arXiv:2009.12077*.
  - [17] J. B. Pendry, P. A. Huidobro, and E. Galiffi, *Optica* **8**, 636 (2021).